



## UNIVERSITY OF GOTHENBURG

This is a copy of an article published in the Stem Cells and Development © 2014 Mary Ann Liebert, Inc.; Stem Cells and Development is available online at: <http://online.liebertpub.com>.

Citation for the published paper:

Papadimitriou Nikolaos, Thorfve Anna, Brantsing Camilla, Junevik Katarina, Baranto Adad, and Barreto Henriksson Helena. Stem Cells and Development. November 1, 2014, 23(21): 2568-2580. doi:10.1089/scd.2014.0153.

# GUP

Gothenburg University Publications

<http://gup.ub.gu.se>

# Cell Viability and Chondrogenic Differentiation Capability of Human Mesenchymal Stem Cells After Iron Labeling with Iron Sucrose

Nikolaos Papadimitriou,<sup>1,2</sup> Anna Thorfve,<sup>3</sup> Camilla Brantsing,<sup>4</sup> Katarina Junevik,<sup>4</sup> Adad Baranto,<sup>1,2</sup> and Helena Barreto Henriksson<sup>1,2</sup>

For evaluation of cell therapy strategies using human mesenchymal stem cells (hMSCs), it is important to be able to trace transplanted cells and their distribution in tissues, for example, cartilage, over time. The aim of the study was to determine effects on cell viability, traceability, and chondrogenic differentiation of hMSCs after iron labeling with iron sucrose. hMSCs were collected (seven donors, 13–57 years) from patients undergoing spinal surgery. Two subsets of experiments were performed. (1) Iron labeling of hMSCs: 1 mg/mL of Venofer<sup>®</sup> (iron sucrose) was added (16 h) to cultures. hMSCs were examined for uptake of iron sucrose (Prussian blue staining) and cell viability (flow cytometry). (2) Iron-labeled hMSCs (passage 4) ( $n=4$ , pellet mass), 200,000 cells/tube, were cultured (DMEM-HG) with 10 ng/mL TGF $\beta$  and compared with controls (from each donor). The pellets were harvested at days 7, 14, and 28. Real-time PCR, IHC, and histology were used to evaluate SOX9, ACAN, C6S, and COL2A1 expression. Mean number of cells containing iron deposits was 98.1% and mean cell viability was 92.7% (no significant difference compared with unlabeled control cells). Pellets containing iron-labeled cells expressed COL2A1 on protein level (all time points), in similar levels as controls, and glycosaminoglycan accumulation was observed in iron-labeled pellets (day 14 or day 28). Results were supported by the expression of chondrogenic genes *SOX9*, *ACAN*, and *COL2A1*. The results in vitro indicate that iron sucrose can be used as a cell tracer for evaluation of cellular distribution in vivo after transplantation of MSCs and thus contribute with important knowledge when exploring new treatment strategies for degenerated cartilaginous tissues.

## Introduction

AT PRESENT TIME, regenerative medicine is a rapidly increasing research field worldwide. In this field, different types of cell therapy applications involving mesenchymal stem cells (MSCs) are under investigation and some applications are already in clinical use [1,2]. Currently, both local and systemic administration applications are used to transplant the MSCs to different organs [1,3–5].

In recent years, stem-cell-therapy-based methods have been discussed as alternative or complementary treatment options for cartilaginous tissue disorders, including intervertebral disc (IVD) degeneration. In general, cartilage is considered to lack or has a poor capacity of self-repair. However, in the IVD, minor self-repair processes have been observed, especially in the outer rings of the annulus fibrosus (AF) [6–8]. In the inner part of the AF and in the nucleus pulposus, no clear regeneration capacity has been

reported [8,9]. For the evaluation of new cell therapy strategies, for example, transplantation of MSCs into degenerated IVDs, it would be of interest to be able to trace the transplanted cells in order to learn how the transplanted MSCs adapt to their new environment. It would be an advantage to be able to examine localization, migration, and function of the transplanted cells and to examine the transplanted cells and their distribution in the IVD tissue of the recipient. However, there is a gap of knowledge regarding the effects of iron labeling on MSCs, regarding cell viability, traceability, and the MSC differentiation capability into the chondrogenic lineage. Further, the major part of fluorescent cell tracers is only traceable for a short time period and not approved for clinical use. Iron is important in several physiological functions in mammals, including oxygen transfer. It is an important cofactor in several enzymes in a variety of different organisms, animals, as well as in plants. In humans, iron deposition mainly takes place in erythrocytes and

<sup>1</sup>Department of Orthopaedics, Institute of Clinical Sciences, Sahlgrenska Academy, University of Gothenburg, Gothenburg, Sweden.

<sup>2</sup>Department of Orthopaedics, Sahlgrenska University Hospital, Gothenburg, Sweden.

<sup>3</sup>Department for Biomaterials, Institute of Clinical Sciences, Sahlgrenska Academy, Gothenburg University of Gothenburg, Gothenburg, Sweden.

<sup>4</sup>Department of Clinical Chemistry and Transfusion Medicine, Institute of Biomedicine, Sahlgrenska Academy, University of Gothenburg, Gothenburg, Sweden.

myocytes by binding of iron to hemoglobin and myoglobin, respectively. The total-body iron content of an adult human ranges from 2 to 4 g, where about two-third of this amount is bound to circulating hemoglobin molecules and one-third is stored in the reticuloendothelial system (liver, spleen, and bone marrow) [10,11]. Only about 0.1% of the total iron pool is present in the peripheral blood circulation (plasma) where it is bound to transferrin, an 80-kDa glycoprotein that is synthesized in the liver. The  $\text{Fe}^{3+}$ -transferrin complex is taken up by cells by active transport over the cell membrane [10,12,13]. Other mechanisms of uptake of iron compounds over the cell membrane into the cytoplasm include endocytosis and phagocytosis [10,12,14].

Previously, superparamagnetic iron oxides (SPIOs; *eg*, Endorem<sup>®</sup>) that are nontoxic have been used clinically for the detection of tumor metastases in the lymphatic system with the use of magnetic resonance imaging (MRI). Further, SPIOs have been used for labeling of cells in *in vitro* (human and animal cells) [14–17] and *in vivo* experiments (animal models) [14,18–20]. It has been demonstrated that SPIOs do not influence MSC differentiation into the osteogenic and/or adipogenic lineage [19,21–23]. The SPIO Endorem, a clinically approved SPIO nanoparticle cell tracer, is no longer commercially available on the market. There are limited clinically approved iron nanoparticles that can be used for evaluation of human cell therapies. This makes it interesting to investigate other nontoxic iron compounds as important tools for and potential cell tracers *in vitro* and in animal models prior to development of human cell therapies. If a good outcome is obtained in preclinical experiments, then such a cell tracer may potentially be used in cell therapy applications for humans. In this study, the potential capability of iron sucrose (Venofer<sup>®</sup>) to be used as a cell tracer was investigated. Venofer<sup>®</sup> is a pharmaceutical clinically approved drug commonly used for patients with iron deficiency [11,24] and the potential capability of this iron compound to be used as a cell tracer was investigated. Venofer consists of iron (III)-hydroxide cores that are superficially surrounded by a large number of noncovalently bound sucrose molecules resulting in a molecular complex with the molecular mass of ~34–60 kDa [25]. The iron in this molecular complex is bound in a similar structure as physiologically occurring ferritin (intracellular storage form of iron in humans). Most cell types (mammalian) have transferrin receptors (CD71) that bind to the iron–transferrin molecule. The transferrin–iron complex is then incorporated into the cytosol by endocytosis [10,26] and stored in the cytosol and mitochondria as ferritin [12,26].

For induction of chondrogenic differentiation of MSCs, the pellet mass three-dimensional (3D) cell culture system was used. This 3D cell culture system is commonly used [15,27] for the differentiation of MSCs into chondrocytes and/or chondrocyte-like cells [15,28]. The pellet mass cell culture system provides an essential microenvironment for chondrocyte differentiation and mimics several different phases in chondrogenesis [28,29]. It has been reported that cartilage formation in pellet mass cultures shares similarities with native cartilage regarding, for example, gene expression, cellular distribution, and extracellular matrix (ECM) composition [30,31].

For MSC profiling and monitoring of differentiation of the MSCs, a set of accepted markers for MSCs was used: CD105 (endoglin), a transmembrane cell surface protein as-

sociated with, for example, human bone marrow stem cells [32–34], and CD166 (ALCAM), a transmembrane glycoprotein that is a member of the immunoglobulin super family of proteins, commonly used in MSC profiling [35–37]. Further, the MSCs should be able to differentiate into osteoblasts, chondrocytes, and adipocytes under standard differentiation *in vitro* conditions [27,33,36,38]. Sex determining region Y-box 9 (SOX9) is a transcription factor and a key regulator in chondrogenesis. SOX9 is expressed during the chondrogenesis and, under the influence of SOX9, the prechondrocytes start to produce collagen type II, which is a major component of the ECM in cartilage [39–41]. Proteoglycans, such as aggrecans, are common components of the ECM that bind to glycosaminoglycans. The most commonly found glycosaminoglycan in mature cartilage is chondroitin-4-sulfate. Chondroitin-6-sulfate (C6S) is a glycosaminoglycan present in newly synthesized ECM of cartilaginous tissues [42–45].

The aim of the study was to determine the effects of labeling with iron sucrose on cell viability and chondrogenic differentiation of human MSCs.

## Materials and Methods

### *Human cells, isolation of human MSCs, and monolayer cultures*

An overview of the experimental design and analyses is shown in Fig. 1.

All experiments were approved by the regional human ethics committee, Vastra Gotaland region, Sweden (ethical permission number 532-04) and the samples were collected after informed consent was obtained from all the patients.

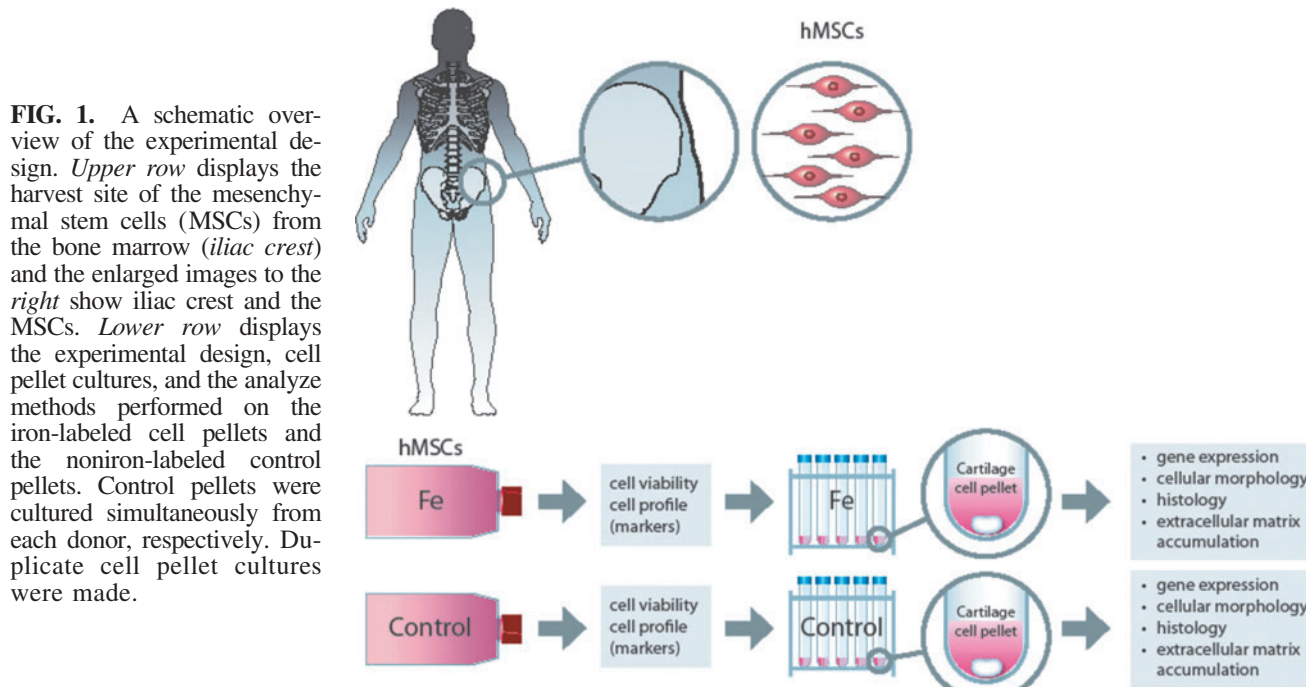
MSCs were collected by bone marrow aspiration (iliac crest) during surgery from seven donors and were isolated from the bone marrow aspirate by centrifugation in cell preparation tubes (Ficoll; Becton Dickinson). The MSCs were thereafter seeded in cell culture flasks (NUNC) at the concentration of  $200 \times 10^3/\text{cm}^2$  and expanded in Dulbecco's modified Eagle's medium, with low-glucose (DMEM-LG) (Invitrogen). The medium was supplemented with 2 mM L-glutamine (Gibco), 100 U/mL/0.1 mg/mL penicillin/streptomycin (PEST; PAA Laboratories), 10 ng/mL  $\beta$ -fibroblast growth factor (Invitrogen), and 10% human serum. The cells were cultured in an incubator (37°C, 7%  $\text{CO}_2$ , 93% air). At 90% confluence in the cell cultures, the MSCs were detached using trypsin/ethylenediaminetetraacetic acid solution (Invitrogen), reseeded at the concentration of  $15 \times 10^3/\text{cm}^2$ , and thereafter expanded to passage 4.

### *Flow cytometry analysis: human MSC profiling*

In order to verify the phenotype of the MSCs, the MSCs were analyzed by flowcytometry for expression of the markers CD105, CD166, CD34, and CD45 expression using fluorescein-, phycoerythrin and peridin conjugated antibodies (Ancell). The instrument used for analysis was an FACSaria flowcytometer (BD Biosciences).

### *Iron labeling of human MSCs*

The MSCs (passage 4) were iron labeled as follows: Venofer (20 mg/mL; Luitpold Pharmaceuticals)  $\{[\text{Na}_2\text{Fe}_5\text{O}_8(\text{OH}) \cdot 3(\text{H}_2\text{O})]n \cdot m(\text{C}_{12}\text{H}_{22}\text{O}_{11})\}$ ; iron sucrose, a brown, sterile,



aqueous solution was used for labeling the MSCs. Cell media were removed from the cell cultures, the cells were subsequently washed with DMEM-LG (without serum), and thereafter serum-free DMEM-LG with 1 mg/mL Venofer (iron sucrose) was added to the human MSC (hMSC) cultures. The hMSC cultures were then incubated for 16 h in 37°C, 7% CO<sub>2</sub>, and 93% air.

The dose of 1 mg/mL Venofer was used in the iron labeling of MSCs, which was based on previous studies for iron labeling of cells in cultures [15,46]. For simplicity reasons, the iron sucrose labeling will be hereafter referred to as iron labeling in the text.

#### Cell viability in cell cultures after iron labeling

Briefly, the cells (5,000 cells per donor) were analyzed for cell viability by incubation for 10 min with 7-aminoactinomycin solution (BD Biosciences) according to the manufacturer's instructions and thereafter analyzed by flow cytometry using an FACSaria instrument (BD Biosciences).

#### Cytospin preparations

MSCs (in passage 4) were detached, 50 µL of cell suspension from each donor was placed in sample chambers with filters and object glasses, and thereafter the cytopsin preparations were centrifuged using a Cytospin 2 instrument (Thermo Fisher/Shandon). Duplicate cytopsin sample preparations were made from each donor. The object glass with the spun-down cells was then gently air dried, stained, and investigated for iron deposits present in the cells using the Prussian blue reaction/staining (Mallory's method), which was performed according to standard protocols [47,48]. The number of cells containing iron deposits was counted using a light microscope NIKONEclipse600 (Nikon) and NIS-elements software. Negative controls were noniron-labeled cells that were analyzed according to the same protocol described previously.

#### Pellet mass cell cultures

After expansion in monolayer, iron-labeled MSCs from four donors (A–D, passage 4) were cultured in the pellet mass culture system [28]. For the pellet cultures, 200,000 cells were pipetted into polypropylene conical tubes (15 mL) containing 0.5 mL of a defined chondrogenic medium consisting of Dulbecco's modified Eagle's medium, with high-glucose (DMEM-HG) (PAA Laboratories) supplemented with 5.0 µg/mL linoleic acid (Sigma-Aldrich), insulin, transferrin, and selenium (Life Technologies); 1.0 mg/mL human serum albumin (Equitech-Bio); 10 ng/mL transforming growth factor (TGF)- $\beta$ 1 (R&D Systems); 10<sup>-7</sup> M dexamethasone (Sigma Aldrich); 14 µg/mL ascorbic acid (Sigma Aldrich); and 1% PEST (PAA Laboratories). The cells were centrifuged at 500 g for 5 min and cultured in an incubator (37°C, 7% CO<sub>2</sub>, 93% air) and the medium was changed twice a week. Duplicate pellet cultures were made and the pellets were harvested after 7, 14, and 28 days. Controls were simultaneously cultured, noniron-labeled pellets from the same donors ( $n=4$ ).

#### Preparation of cell pellets for histology and immunohistochemistry

The cell pellets were placed in 4% formaldehyde (Histolab Products AB) and imbedded in paraffin and 5–7-µm sections were prepared. Paraffin sections were deparaffinized with xylene for 2×10 min and rehydrated in 99%, 95%, and 70% ethanol for 5 min in each solution prior to analysis.

#### Immunohistochemistry

**SOX9.** Sections of the pellets were deparaffinized and rehydrated as described in the section "Preparation of cell pellets for histology and immunohistochemistry."

For analysis of SOX9, an antigen retrieval step using 0.1 M sodium citrate buffer (pH 6.0) for 20 min at 90°C was used. Samples were blocked with 2% bovine serum albumin (BSA;



Sigma) and 0.5% Triton-X100 diluted in phosphate-buffered saline (PBS) and thereafter a mouse anti-SOX9 antibody (Abcam), diluted 1:500 in PBS-containing blocking solution, was applied to the sections, which thereafter were incubated overnight at 4°C. The primary antibody was visualized using a goat anti-mouse secondary Alexa fluor 546-conjugated antibody (Invitrogen), diluted 1:250, and it was applied to the sections which thereafter were incubated at room temperature (RT) for 2 h. Sections were mounted with Prolong gold antifade media (Invitrogen) containing the nuclear staining compound 4,6 diamino-2 phenylindole (DAPI).

**Cell counting: SOX9.** Semiquantification was performed of the SOX9-positive cells in pellets. The SOX9-positive cells (yellow color) were counted in one pellet section from each pellet in a defined area measured in the center of the pellets consisting of one field of view (40× objective). Each positive-counted cell was marked with an X (cell count function) in order to avoid double counts using the software NIS elements BR 3.0 (Nikon) and a fluorescence microscope NikonEclipse600 (Nikon).

**Collagen2A1.** Immunohistochemical analyses for detection of collagen2A1 accumulation in pellets were performed. Samples were digested with 8,000 U/mL of hyaluronidase (Sigma Aldrich) in PBS (pH 7.4) for 1 h at 37°C and thereafter blocked with 3% BSA (Sigma-Aldrich). Sections were labeled with goat anti-collagen2A1 antibody (Santa Cruz) diluted 1:100 in PBS containing 3% BSA (Sigma-Aldrich) and incubated overnight at 4°C. The primary antibody was visualized using an anti-goat secondary antibody, horseradish peroxidase conjugated (Jackson Laboratory), diluted 1:200, and sections were incubated at RT for 2 h. An enhancement step was performed using the TSA-direct Cy-3 kit (Perkin Elmer) according to the manufacturer's instructions. Sections were mounted with Prolong gold antifade media (Invitrogen) containing the nuclear staining compound 4,6 diamino-2 phenylindole (DAPI).

**C6S.** Sections of the pellets were deparaffinized and rehydrated as described under the section; preparation of cell pellets for histology and immunohistochemistry.

For analysis of C6S, an antigen-retrieval step using 0.05 U/mL of chondroitinase ABC (Sigma Aldrich) was performed for 1 h at 37°C, blocked with 3% BSA (Sigma-Aldrich), and thereafter a mouse anti-C6S antibody (Millipore), diluted 1:100 in PBS containing 3% BSA (the antibody is directed toward the residual molecular epitopes that are detectable after digestion with chondroitinase ABC), was applied to the sections which thereafter were incubated overnight at 4°C. The primary antibody was visualized using a goat anti-mouse secondary Alexa fluor 488-conjugated antibody (Invitrogen), diluted 1:250, and it was applied to the sections which thereafter were incubated at RT for 2 h.

Sections were mounted with Prolong gold antifade media (Invitrogen) containing the nuclear staining compound 4,6 diamino-2 phenylindole. The sections were then examined for C6S expression using a fluorescence microscope Nikon-Eclipse600 (Nikon) and NIS-elements software. Negative controls were isotype controls and/or sections incubated with the primary antibody omitted.

#### *Histology of pellets: ECM accumulation and iron staining*

The sections were stained for glycosaminoglycans by the Alcian blue Van Gieson staining method [49,50] and for

iron deposits as earlier and examined by light microscopy using a microscope NikonEclipse600 (Nikon).

#### *Isolation of RNA*

Two to three cell pellets consisting of iron-labeled or noniron-labeled cells were pooled and placed in RNA later<sup>®</sup> (Qiagen) and thereafter frozen at −80°C until further analysis. Isolation of RNA was performed by homogenization in RLT lysis buffer (Qiagen) using a Tissue lyser instrument (Qiagen) and the standard protocol for RNeasy Mini Kit (Qiagen).

#### *Quantitative real-time polymerase chain reaction analysis*

cDNA was prepared from the pellets from a minimum of 72 ng of total human ( $n=4$ ) RNA using TaqMan<sup>®</sup> Reverse Transcription reagents and random hexamer primers (Life Technologies). The temperature program during cDNA synthesis was 25°C for 10 min, 37°C for 120 min, and 85°C during 5 s. Preamplifications were performed with TaqMan PreAmp Master Mix for all samples (Life Technologies). Quantitative polymerase chain reaction (qPCR) analysis was performed using the instrument ABI7900HT (Life Technologies). The following human TaqMan gene expression assays were used: ACAN (proteoglycan, ECM component) (Hs00153936\_m1), CD105 (marker for MSCs) (Hs00923996\_m1), CD166 (marker for MSCs) (Hs00977641\_m1), SOX9 (chondrogenic lineage marker) (Hs00165814\_m1), COL2A1 (chondrogenic marker for early ECM synthesis) (Hs00156568\_m1), and COL2B (chondrogenic marker, mature ECM) (Hs01064869\_m1). qPCR was performed in 20-μL volume for each sample with 10 μL of 2× TaqMan Gene Expression Master Mix and 1 μL of 20× Gene Expression Assays, with temperature program as follows: 50°C for 2 min, 95°C for 10 min succeeded by 95°C for 15 s and 60°C for 1 min during 40 cycles. Samples were analyzed in duplicates and the relative gene expression was evaluated by the  $2^{-\Delta\Delta Ct}$  method in GenEx Enterprise 5.2.3.13 (MultiD Analyses). Reference genes used in the analysis were CYCLOPHILIN A (Hs99999904\_m1) and CREBBP (Hs00231733\_m1).

However, since iron molecular compounds, for example, FeCl<sub>3</sub>, have been reported to inhibit the activity of polymerases and may therefore disturb the qPCR analysis (and in vivo) [51,52], the gene results are presented only as detected (D/D) or not detected (ND/ND). CT values above 37 were considered not detected (ND/ND).

#### *Statistical analysis*

Cell viability of the iron-labeled cells and SOX9 expression in the pellets were examined and compared with noniron-labeled control cells from each donor using the Student's *t*-test. The profile of MSC surface markers—CD105, CD166, CD45, and CD34—was analyzed and compared with controls using the Student's *t*-test. A *P*-value <0.05 was considered statistically significant when comparing iron-labeled cells with noniron-labeled control cells from the same donor.

## **Results**

#### *Flow cytometry: MSC markers*

Prior to start of pellet cultures, the cells were iron labeled for 16 h and thereafter the cells were tested for a panel of

accepted MSC markers: CD105 and CD166 (markers for MSCs), CD34 (marker for hematopoietic stem cells), and CD45 (marker for leukocytes). In passage 4, the mean values of MSC markers of the cells were as follows: nonlabeled control cells, CD105, 96.0%; CD166, 90.2%; CD45, <10%; and CD34, <10% ( $n=4$ ), and for the iron-labeled cells, CD105, 70.7%; CD166, 71.9%; CD45, <10%; and CD34, <10% ( $n=4$ ). There was a significant difference in the CD105 expression ( $P<0.05$ ) while no significant difference was found in the CD166 ( $P=0.10$ ), CD45 ( $P=0.16$ ), or CD34 ( $P=0.25$ ) expression between the iron-labeled cells when compared with the noniron-labeled control cells (Fig. 2A).

#### Flow cytometry: cell viability

The mean cell viability for iron-labeled cells was 92.7% and 94.6% for the noniron-labeled control cells (no signif-

icant difference when compared with the noniron-labeled control cells) at start of the pellet cultures ( $n=7$ ,  $P=0.26$ ) (Fig. 2B, C).

#### Detection of iron deposits in MSCs after iron labeling

After iron labeling of the cytospin sample cell preparations, the mean number of cells containing iron deposits was 98.1% ( $n=7$ ). Controls of noniron-labeled MSCs showed no staining ( $n=7$ ) (Fig. 3).

#### Traceability of iron deposits in the cell pellets

In the iron-labeled cell pellets, deposits of iron compounds were clearly visible as intense blue granulae in the cytosol of the cells and the intracellular iron deposits were relatively evenly distributed in the cell pellets at all time

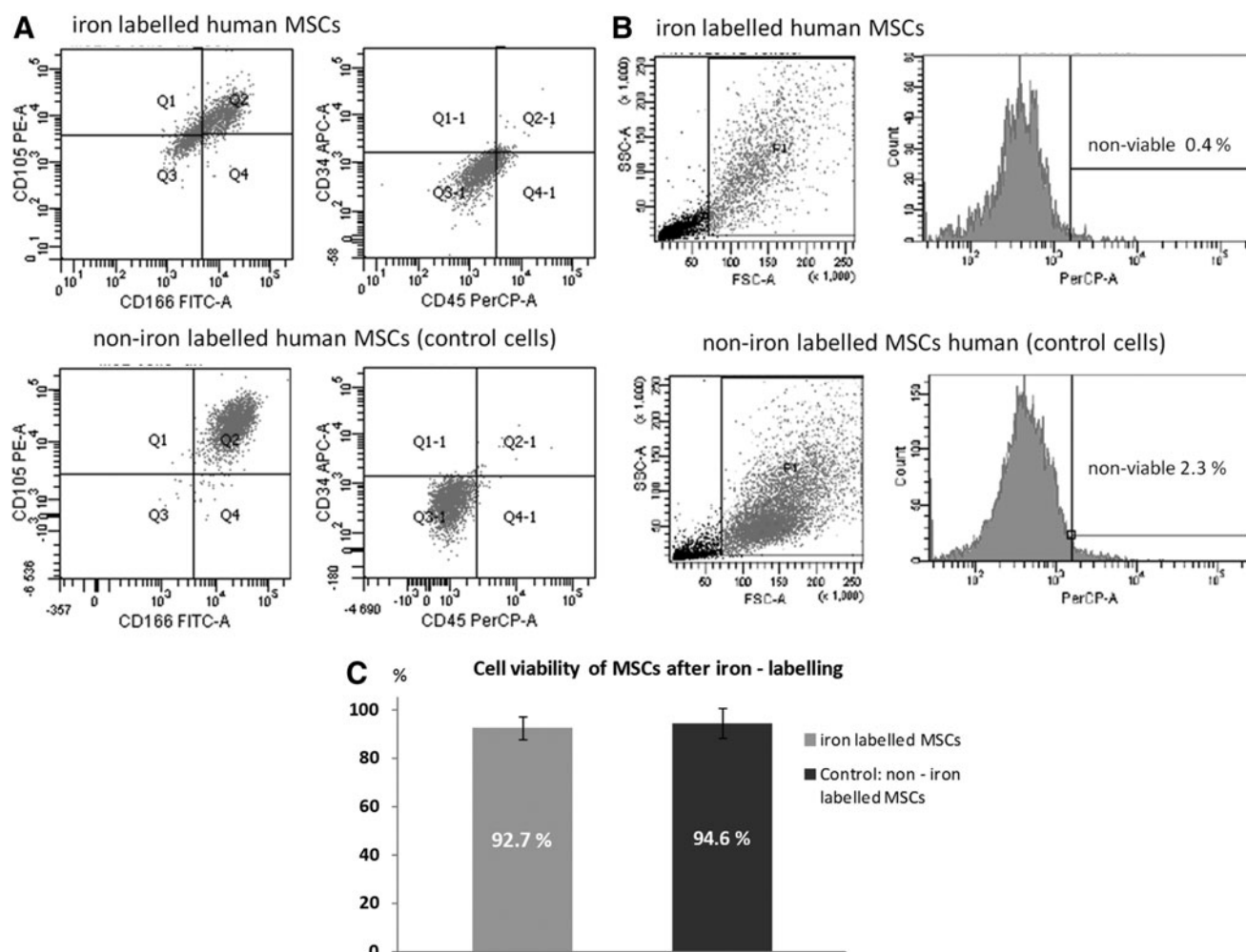


**FIG. 2.** (A) Flow cytometry results displaying the MSC profile of one donor (male, age 51 years); double-positive cells for the stem cell markers CD105 and CD166 and cells negative for CD45 and CD34. *Upper row* displays the flow cytometry results from the iron-labeled cells and in the *lower row* the noniron-labeled control cells are displayed. (B) Histograms of flow cytometry results of the 7-aminoactinomycin staining for cell viability from one donor (female, age 45 years) (*upper row*), displaying the cell viability results for the iron-labeled human MSCs that was 99.6% (nonviable cells: 0.4%) and for the noniron-labeled human control MSCs that was 97.7% (nonviable cells: 2.3%) (*lower row*) and (C) bar graph displaying the mean cell viability  $\pm$  2 standard deviation of donors ( $n=7$ ). There was no significant difference ( $P=0.26$ ) of cell viability of the iron-labeled human MSCs when compared with the noniron-labeled control cells.



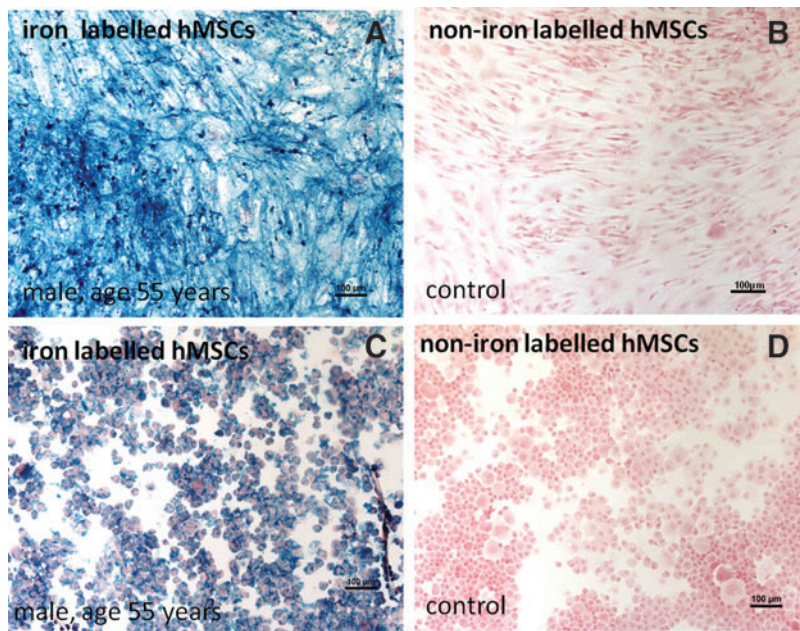


**FIG. 3.** Images of monolayer cultures and cytopsin preparations of one representative donor (male, age 55 years) of (A) iron-labeled cells in monolayer with clearly visible iron granulae/deposits (blue) and (B) noniron-labeled control cells in monolayer culture, (C) iron-labeled cells in cytopsin preparations with clearly visible iron granulae/deposits (blue) in the cytoplasm and (D) cytopsin preparations of noniron-labeled control cells. The mean number of cells containing iron deposits in the iron-labeled cell samples (cytopsin preparations) was 98.1%. Negative controls showed no staining. Staining: Prussian blue reaction/staining (Mallory's method).

points. The iron-labeled and the noniron-labeled control pellets displayed rounded or nonrounded morphological shapes ( $n=4$ ) (Fig. 4).

#### Expression of chondrogenic lineage marker SOX9

Cells expressing SOX9 were detected in the iron-labeled pellets at all the time points (4/4 donors). The SOX9 expression was more pronounced in the cell pellets at the earlier time points, day 7 and/or day 14 in the iron-labeled pellets and in the noniron-labeled control pellets, compared with cell pellets at day 28 in both groups. No statistical differences were found when comparing the number of

SOX9-positive cells in all donors per pellet/section in iron-labeled pellets to controls at any time point (day 7:  $P=0.10$ , day 14:  $P=0.34$ , and day 28:  $P=0.18$ ) (Fig. 5).

#### Analysis of extracellular matrix components: protein level

**Collagen2A1.** Expression of collagen2A1 was detected in the iron-labeled pellets at all the time points, peaking at day 28 (4/4 donors) in comparable levels as controls. In the noniron-labeled control pellets, collagen2A1 expression was detected at all the time points (4/4 donors) (Fig. 6).

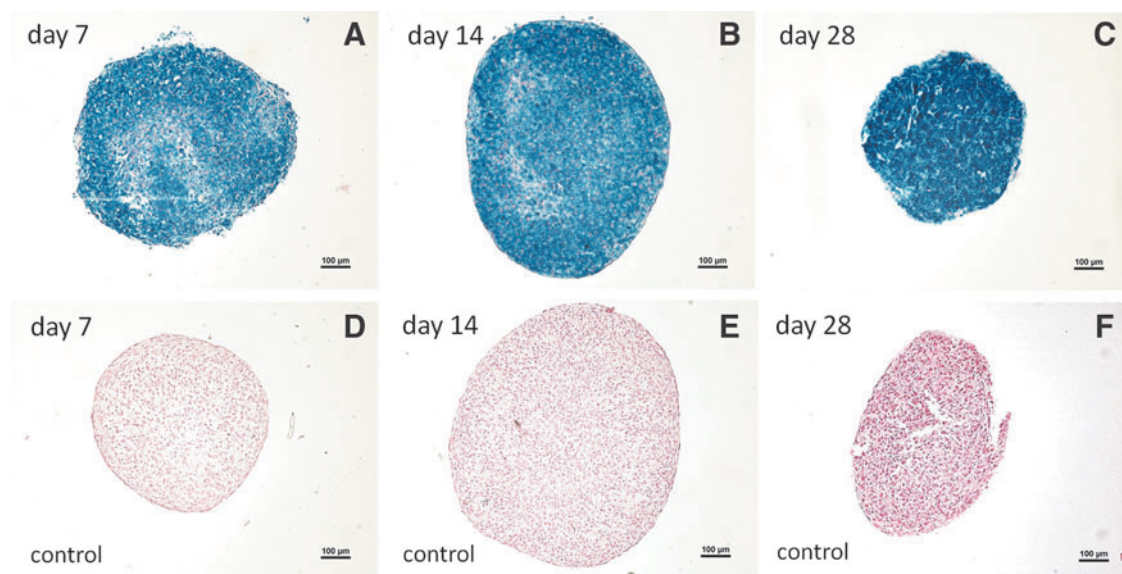


**FIG. 4.** Images in upper row display iron-labeled cell pellets (blue color) from (A) day 7, (B) day 14, and (C) day 28 from one of the donors (male, age 35 years) and in the lower row (D–F) the noniron labeled control pellets are displayed from the same time points (same donor). Staining: Prussian blue reaction/staining (Mallory's method).

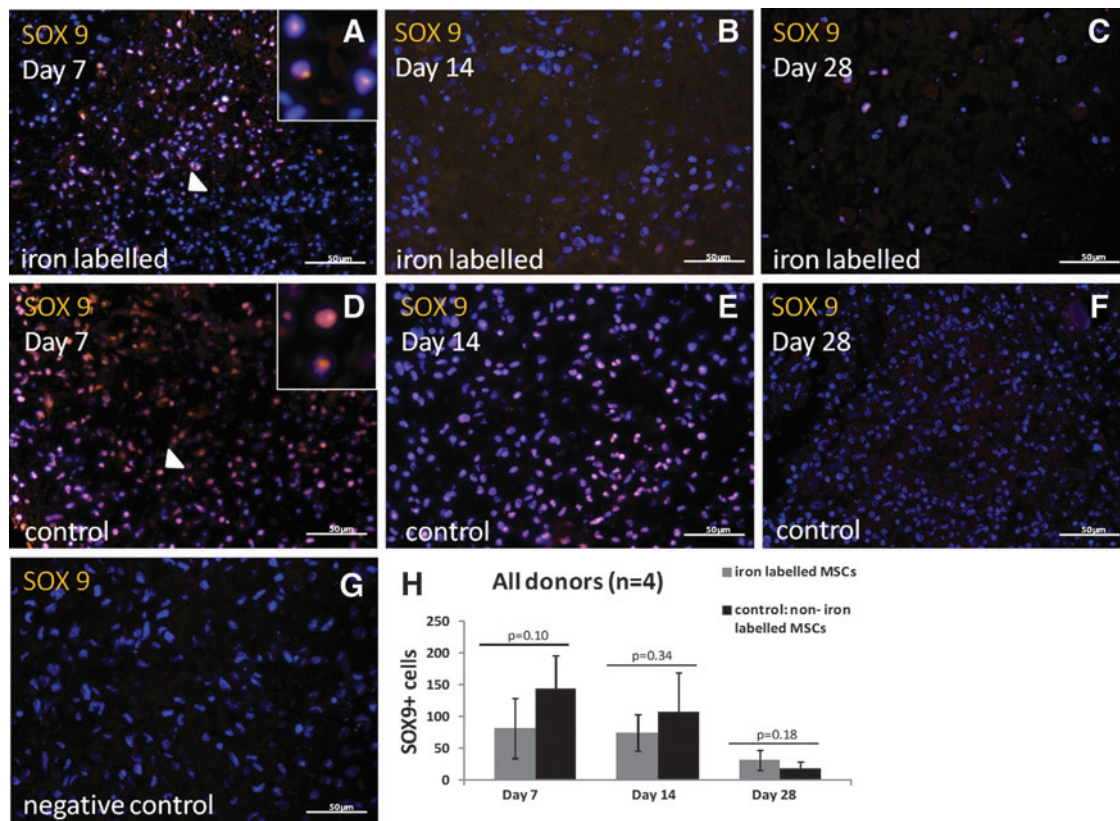


**FIG. 5.** Images taken from center part of the pellets of immunohistochemical stainings of sex determining region Y-box 9 [SOX9, yellow color, nuclei stained with 4,6 diamino-2 phenylindole (DAPI, blue)] from one of the donors (male, age 35 years). (A–C) iron-labeled pellets (days 7–28), in image (A) an enlarged image of SOX9 positive cells (white arrow) is displayed in upper right corner, (D–F) noniron-labeled control pellets (days 7–28), in image (D) an enlarged image of SOX9 positive cells (white arrow) is displayed in upper right corner, (G) negative control, and (H) bar graph displaying SOX9-positive cells detected in the iron-labeled cell pellets (gray bars) and noniron-labeled cell pellets (controls, black bars) from the donors. Each bar represents the cell number  $\pm$  standard error of the means from two pellets/sections. In the graph, the total cell number of SOX9-positive cells in each time point from all the donors is displayed. No statistical differences were found when comparing the total number of SOX9-positive cells of all donors per pellet/section in the iron-labeled pellets to the controls at any time points. There was a more pronounced positive SOX9 expression observed in the cell pellets at the earlier time points (day 7 and/or day 14) in the iron-labeled pellets and in the noniron-labeled control pellets compared with cell pellets at day 28 in both groups.

**Glycosaminoglycans: C6S expression.** Expression of C6S was detected in 3/4 donors at the time points day 14 (2/4 donors) and day 28 (4/4 donors) in the iron-labeled cell pellets.

In noniron-labeled control pellets, C6S expression was detected at day 7 (2/4 donors) and day 14 (2/4 donors) and at day 28 (4/4 donors) (Fig. 7).

**Glycosaminoglycans: histology.** The MSCs formed cell pellets with various rounded shapes in the pellet mass cell cultures and an increase in pellet size was macroscopically observed in the cell pellets over time. In the iron-labeled cell pellets at day 14 (2/4 donors) and day 28 (3/4 donors), a weak positive staining for glycosaminoglycan accumulation was detected. In the noniron-labeled control pellets, a low positive staining for glycosaminoglycan accumulation was detected at day 14 (2/4 donors) and at day 28 (4/4 donors) (Fig. 8).

#### Gene expression of MSCs

Gene expression of the MSC markers *CD105* and *CD166* was detected in the iron-labeled cell pellets (donors A–D,  $n=4$ ); *CD105* was detected at day 7 and day 14 (4/4 donors) and at day 28 (3/4 donors). *CD166* gene expression was

detected at days 7 (4/4 donors), 14, and 28 (3/4 donors). In the noniron-labeled control cell pellets ( $n=4$ ), gene expression of *CD105* was detected at all time points (4/4 donors) and *CD166* gene expression was detected at the time point day 7 (4/4 donors) and days 14 and 28 (3/4 donors). In the iron-labeled pellets ( $n=4$ ), gene expression of the chondrogenic lineage marker *SOX9* was detected at days 7 and 14 (3/4 donors) and at day 28 (2/4 donors). In the noniron-labeled control cell pellets, *SOX9* expression was found at days 7 (4/4 donors), 14, and 28 (3/4 donors). Gene expression of the chondrogenic ECM marker *COL2A1* was detected in iron-labeled cell pellets at days 7 (1/4 donors), 14, or 28 (2/4 donors). *COL2A1* gene expression was detected in noniron-labeled control pellets at day 7 (3/4 donors) and at day 28 (3/4 donors). *COL2B* (chondrogenic marker, mature ECM) gene expression was detected in the iron-labeled cell pellets at day 14 or at day 28 (2/4 donors). *COL2B* gene expression was detected in noniron-labeled control pellets at day 7 (1/4 donors) and at day 28 (3/4 donors). In the iron-labeled pellets, gene expression of *ACAN* was detected at day 7 (3/4 donors), day 14, or at day 28 (2/4 donors). In the noniron-labeled control pellets,



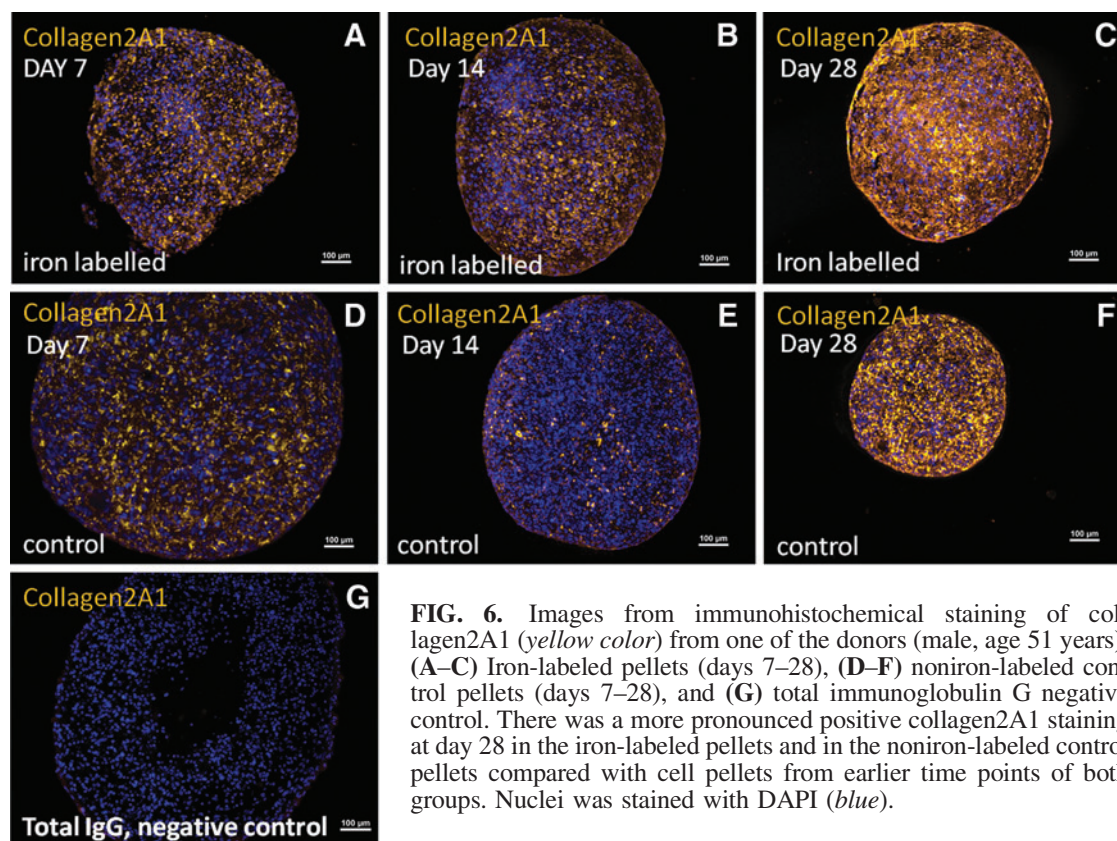


**FIG. 6.** Images from immunohistochemical staining of collagen2A1 (yellow color) from one of the donors (male, age 51 years). (A–C) Iron-labeled pellets (days 7–28), (D–F) noniron-labeled control pellets (days 7–28), and (G) total immunoglobulin G negative control. There was a more pronounced positive collagen2A1 staining at day 28 in the iron-labeled pellets and in the noniron-labeled control pellets compared with cell pellets from earlier time points of both groups. Nuclei was stained with DAPI (blue).

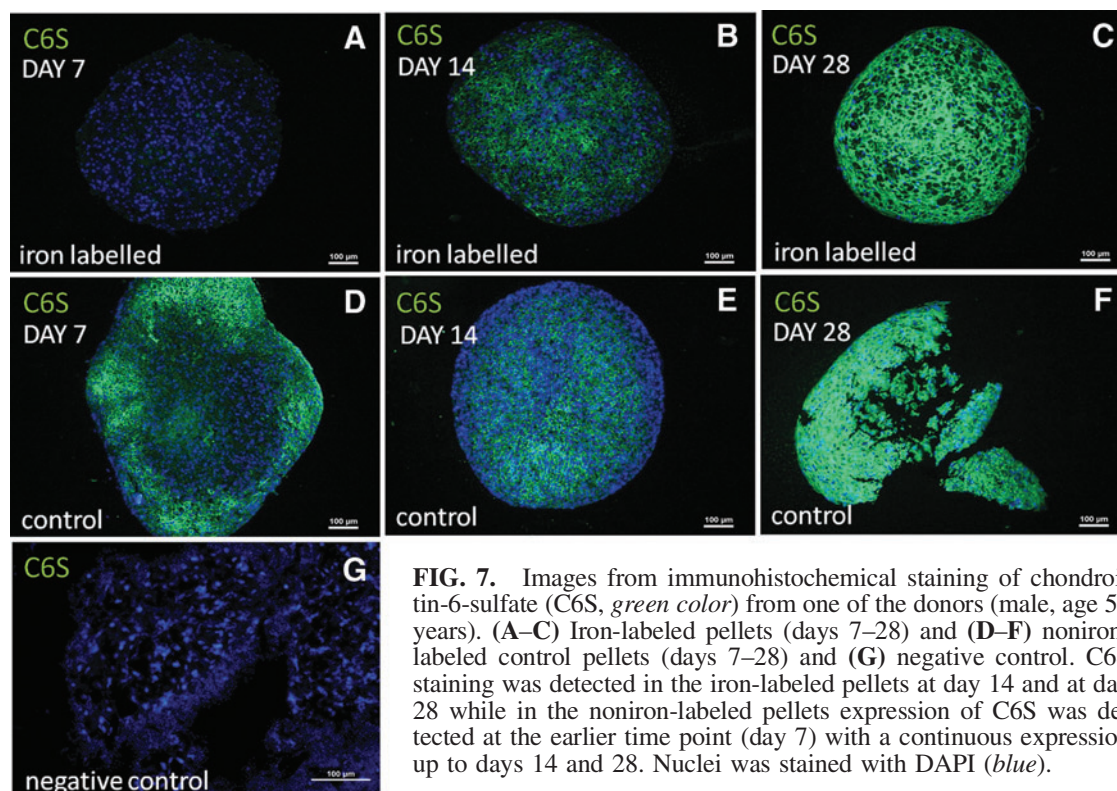


**FIG. 7.** Images from immunohistochemical staining of chondroitin-6-sulfate (C6S, green color) from one of the donors (male, age 51 years). (A–C) Iron-labeled pellets (days 7–28) and (D–F) noniron-labeled control pellets (days 7–28) and (G) negative control. C6S staining was detected in the iron-labeled pellets at day 14 and at day 28 while in the noniron-labeled pellets expression of C6S was detected at the earlier time point (day 7) with a continuous expression up to days 14 and 28. Nuclei was stained with DAPI (blue).

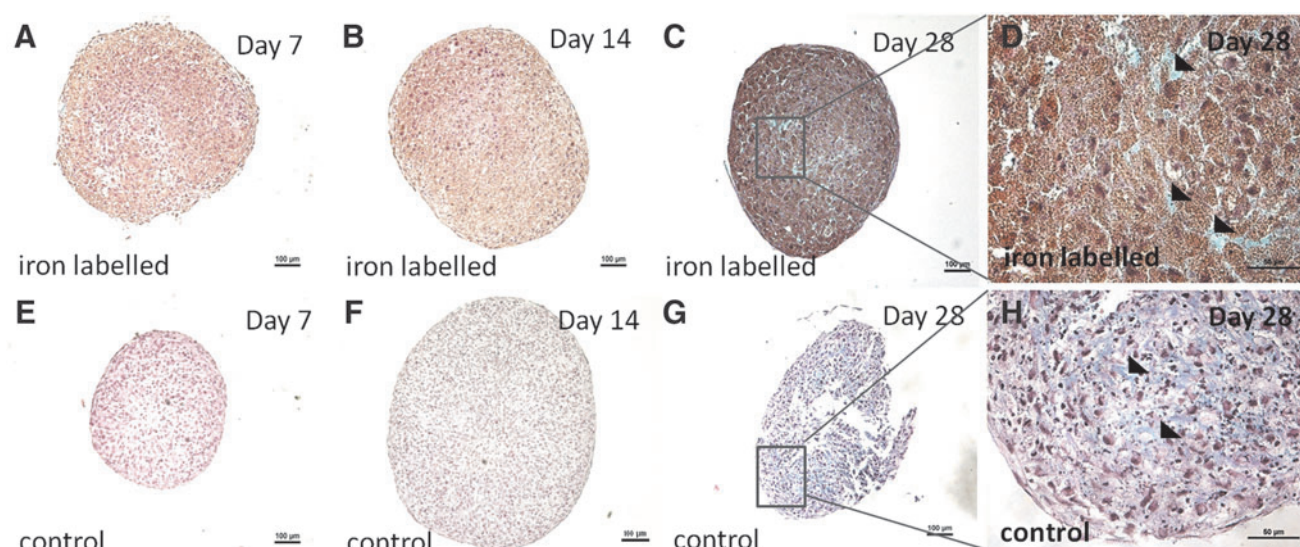


**FIG. 8.** Images from histology staining of glycosaminoglycans (*pale blue*) from one of the donors (male, age 51 years). (A–C) Iron-labeled pellets (days 7–28), (D) a higher magnification of image (C) where glycosaminoglycan accumulation is indicated by *black arrows* (E–G) noniron-labeled control pellets (days 7–28) and (H) a higher magnification of image (G) where glycosaminoglycan accumulation is indicated by *black arrows*. A week positive staining for glycosaminoglycans was detected at day 28 in the iron-labeled pellets and in the noniron-labeled control pellets. Staining: Alcian blue van Gieson (sulfated glycosaminoglycans appear *blue* and collagens appear *red*).

ACAN was detected at the time points day 7 (4/4 donors), 14 (2/4 donors), and 28 (3/4 donors) (Table 1).

## Discussion

In this study, the effects of iron labeling on human MSC survival and differentiation into the chondrogenic lineage were investigated. TGF- $\beta$  and a pellet mass culture system were used to induce the differentiation of human MSCs into the chondrogenic lineage. Other factors that have been reported to induce chondrogenic differentiation and ECM accumulation are, for example, biomechanical forces, local cell signaling, and surface topography of the microenvironment [53,54]. Regarding the effect of iron labeling on differentiation of MSCs into the chondrogenic lineage, there are a few reports with divergent data that describe effects [55] on the chondrogenic differentiation [56,57]. However, recent studies have demonstrated that iron labeling does not affect the “stemness” of human bone-marrow-derived MSCs [57,58]. In the present study, after the iron labeling of MSCs, the cell viability was observed to be at similar level as in controls prior to start of the cell pellet cultures. The iron deposits were clearly detectable in the cultured iron-labeled MSC pellets up to day 28 (end point of the study). The results are comparable with previous studies that use iron nanoparticles (SPIOs) for labeling of MSCs in in vitro and animal models [14,15,16,21]. SPIOs are an elegant alternative when it comes to noninvasive cell tracking using MRI. In addition to that, they offer the opportunity of exogenous cell manipulation by magnetic fields for, that is, cell-targeting purposes as demonstrated by El Haj et al. [17]. To the best of our knowledge there are no such agents available for use in humans at the present time. Recently, Thu et al. proposed the off-label use of a combination of three different FDA-approved pharmaceutical compounds (ferumoxytol, heparine, and protamine) for SPIO cell labeling with promising

results [59]. Our results from this study suggest that iron sucrose (Venofer) can be an in-vivo-cell-labeling option with a known, favorable risk profile (considering possible adverse effects such as allergic reactions) for use even in humans—in experimental designs where tissue samples can be acquired for histological examination [17].

In this study, the iron-labeled cells were able to form cartilage-like cell pellets in the pellet mass culture system and the cultured cell pellets were able to differentiate into the chondrogenic-lineage-expressing SOX9 and ECM markers collagen2A1 and C6S on a protein level. Normally, the gene expression precedes the protein expression in time. In the iron-labeled cell pellets, gene expression was detected from days 7 to 28 in the pellets, which supports that the cells were viable and active since gene expression of the investigated genes was detected in these samples (RNA has a short degrading time in vivo). Expression of chondrogenic genes displayed variation between donor samples in the iron-labeled pellets as well as in the nonlabeled control pellets. Presumably, the variation observed in the iron-labeled cell pellets is explained by reports of that iron compounds; for example, FeCl<sub>3</sub> can inhibit or disturb the activity of polymerases by competing for the Mg<sup>2+</sup> binding site at the polymerase molecule [51,52,60]. Mg<sup>2+</sup> is a cofactor for the polymerase enzyme and hence it is necessary for the activity of this enzyme in order to the transcription of DNA or RNA can take place [51,61]. In addition, normal variation in gene expression between pellets can occur between donors and over time. Notwithstanding, the pellets were able to differentiate into the chondrogenic lineage as seen in the observed SOX9 expression (on gene and protein levels). In general, the SOX9 expression (protein level) was slightly lower in the iron-labeled cell pellets compared with the noniron-labeled pellets but no statistical differences were found when comparing the total SOX9 expression of all donors in iron-labeled pellets to controls (Fig. 5).



TABLE 1. EXPRESSION OF THE INVESTIGATED GENES (ALL DONORS,  $n=4$ )—*CD105*, *CD166*, *SOX9*, *COL2A1*, *COL2B*, AND *ACAN*—AT THE DIFFERENT TIME POINTS (DAYS 7–28)

	Day 7	Ctrl day 7	Day 14	Ctrl day 14	Day 28	Ctrl day 28
Donor A (age 49)						
CD105	D//D	D//D	D//D	D//D	D//D	D//D
CD166	D//D	D//D	ND/ND	D//D	D//D	D//D
SOX9	ND/ND	D//D	ND/ND	D//D	D//D	D//D
COL2A1	ND/ND	D//D	ND/ND	ND/ND	D//D	D//D
COL2B	ND/ND	D//D	ND/ND	ND/ND	D//D	D//D
ACAN	D//D	D//D	ND/ND	D//D	D//D	D//D
PPIA	D//D	D//D	D//D	D//D	D//D	D//D
CREBP	D//D	D//D	ND/ND	D//D	D//D	D//D
Donor B (age 55)						
CD105	D//D	D//D	D//D	D//D	D//D	D//D
CD166	D//D	D//D	D//D	D//D	D//D	D//D
SOX9	D//D	D//D	D//D	D//D	ND/ND	ND/ND
COL2A1	D//D	ND/ND	ND/ND	ND/ND	ND/ND	ND/ND
COL2B	ND/ND	ND/ND	ND/ND	ND/ND	ND/ND	ND/ND
ACAN	D//D	D//D	ND/ND	ND/ND	ND/ND	ND/ND
PPIA	D//D	D//D	D//D	D//D	D//D	D//D
CREBP	D//D	D//D	D//D	D//D	D//D	D//D
Donor C (age 35)						
CD105	D//D	D//D	D//D	D//D	D//D	D//D
CD166	D//D	D//D	D//D	D//D	D//D	ND/ND
SOX9	D//D	D//D	D//D	D//D	D//D	D//ND
COL2A1	ND/ND	D//D	ND/ND	ND/ND	ND/ND	D//ND
COL2B	ND/ND	ND/ND	ND/ND	ND/ND	ND/ND	D//D
ACAN	ND/ND	D//D	ND/ND	D//D	ND/ND	D//D
PPIA	D//ND	D//D	D//D	D//ND	D//D	D//D
CREBP	D//D	D//D	D//D	ND/ND	D//D	D//D
Donor D (age 51)						
CD105	D//D	D//D	D//D	D//D	ND/ND	D//D
CD166	D//D	D//D	D//D	ND/ND	ND/ND	D//D
SOX9	D//D	D//D	D//D	ND/ND	ND/ND	D//D
COL2A1	ND/ND	D//D	D//D	ND/ND	ND/ND	D//D
COL2B	ND/ND	ND/ND	D//D	ND/ND	ND/ND	D//D
ACAN	D//D	D//D	D//D	ND/ND	ND/ND	D//D
PPIA	D//D	D//D	D//D	ND/ND	ND/ND	D//D
CREBP	D//D	D//D	D//D	D//D	ND/ND	D//D

The results are presented as detected (D//D, highlighted in *light gray* color) or not detected (ND/ND, highlighted in *dark gray* color).

Further, extracellular matrix components collagen2A1 and C6S were observed on protein level in the pellets especially at the time points days 14 and 28, which was supported by the gene expression data of the same markers. In the iron-labeled pellets, in some of the donors, the gene expression of the chondrogenic genes was somewhat less detectable when compared with the noniron-labeled control pellets, indicating that the iron labeling may influence and/or delay the differentiation into the chondrogenic lineage of the human MSCs.

The flow cytometry results revealed that the stemness of MSCs when iron labeled (in aspects of cell surface marker profile) was slightly altered when compared with the noniron-labeled pellets. It appears as if the cell surface marker profile of the MSCs was affected by the iron labeling procedure since the CD105 expression was found to be significantly lower in the flow cytometry analysis (performed directly after the iron labeling procedure) when compared with the noniron-labeled control cells. No differences were observed for the other investigated markers.

Previously, in an in vitro study with pellet cocultures, a mixture of human MSCs and IVD cells was used in different ratios and iron nanoparticle (Endorem) labeling of one of the cell types (MSCs) was performed [15] and the iron deposits were thereafter detectable for up to 28 days (the latest investigated time point) [15]. In addition, in a recent in vivo study (lapine model), in situ labeling with iron nanoparticles (Endorem) of local cells in the IVD region (niche area adjacent to the epiphyseal plate) was reported where the labeled cells could be traced up to 6 weeks after the in situ labeling and detected distributed as solitary iron-deposit-containing cells within the IVD at relatively far distance from the injection site [62].

Limitations of this study were that a relatively small sample size was used. Data from the qPCR analyses were limited due to the fact that iron compounds most likely influenced/inhibited the activity of polymerases. Further, it is possible that a more pronounced differentiation of the MSCs into the chondrogenic lineage and ECM accumulation in the iron-labeled cell pellets would have been



obtained if the cell pellet cultures would have been maintained in the cell cultures for a longer time period.

## Conclusions

The pharmaceutical compound Venofer, iron sucrose compound, may be suitable as a cell tracer in in vivo studies of distribution of transplanted cells, for example, MSCs. The investigated iron sucrose compound provides a stable detectable signal and was found at all time points during differentiation, which gives it an advantage over other cell tracer compounds, for example, fluorochrome tracers that often lose their signal more rapidly over time.

Further, the cell viability was not affected by the iron labeling procedure while the differentiation into the chondrogenic lineage of the MSCs was to some extent influenced in the iron-labeled cell pellets compared with the controls. Hence, the iron labeling procedure appears to slightly delay the differentiation into the chondrogenic lineage over time. However, it should be mentioned that the labeled cells were able, in any case, to form pellets, indicating a significant residual chondrogenic differentiation capacity. The described iron labeling model in this study can be useful in in vivo models for monitoring of cellular distribution after stem cell transplantation, for example, by histology methods, and thus contribute with important knowledge when exploring new treatment strategies for cartilaginous tissues involving different stem cell therapy applications.

## Acknowledgments

The study was supported with grants from the Swedish Research Council, the Neubergh Foundation, the Hjalmar Svensson Foundation, Sahlgrenska University hospital funds, the Royal Society of Art and Sciences, VINNOVA, and BIOMATCELL VINN Excellence Center of Biomaterials and Cell Therapy, Gothenburg, Sweden.

## Author Disclosure Statement

The authors declare no conflict of interest.

## References

- Horwitz EM, PL Gordon, WK Koo, JC Marx, MD Neel, RY McNall, L Muul and T Hofmann. (2002). Isolated allogeneic bone marrow-derived mesenchymal cells engraft and stimulate growth in children with osteogenesis imperfecta: implications for cell therapy of bone. *Proc Natl Acad Sci U S A* 99:8932–8937.
- Bobis S, D Jarocha and M Majka. (2006). Mesenchymal stem cells: characteristics and clinical applications. *Folia Histochem Cytobiol* 44:215–230.
- Barry FP. (2003). Biology and clinical applications of mesenchymal stem cells. *Birth Defects Res C Embryo Today* 69:250–256.
- Abdallah BM and M Kassem. (2008). Human mesenchymal stem cells: from basic biology to clinical applications. *Gene Ther* 15:109–116.
- Svenberg P, M Remberger, J Svennilson, J Mattsson, K Leblanc, B Gustafsson, J Aschan, L Barkholt, J Winiarski, P Ljungman and O Ringden. (2004). Allogeneic stem cell transplantation for nonmalignant disorders using matched unrelated donors. *Biol Blood Marrow Transplant* 10:877–882.
- Humzah MD and RW Soames. (1988). Human intervertebral disc: structure and function. *Anat Rec* 220:337–356.
- Melrose J, SM Smith, ES Fuller, AA Young, PJ Roughley, A Dart and CB Little. (2007). Biglycan and fibromodulin fragmentation correlates with temporal and spatial annular remodelling in experimentally injured ovine intervertebral discs. *Eur Spine J* 16:2193–2205.
- Smith JW and R Walmsley. (1951). Experimental incision of the intervertebral disc. *J Bone Joint Surg Br* 33-B:612–625.
- Melrose J, P Ghosh, TK Taylor, A Hall, OL Osti, B Vernon-Roberts and RD Fraser. (1992). A longitudinal study of the matrix changes induced in the intervertebral disc by surgical damage to the annulus fibrosus. *J Orthop Res* 10:665–676.
- Vander ASJ and D Luciano. (ed.). (1987). *Human Physiology. The Mechanisms of Body Function*, 4th edn. McGraw-Hill, Inc., Singapore.
- Kosch M, U Bahner, H Bettger, F Matzkies, M Teschner and RM Schaefer. (2001). A randomized, controlled parallel-group trial on efficacy and safety of iron sucrose (Venofer) vs iron gluconate (Ferlecit) in haemodialysis patients treated with rHuEpo. *Nephrol Dial Transplant* 16:1239–1244.
- Lawen A and DJ Lane. (2013). Mammalian iron homeostasis in health and disease: uptake, storage, transport, and molecular mechanisms of action. *Antioxid Redox Signal* 18:2473–2507.
- Prus E and E Fibach. (2008). Flow cytometry measurement of the labile iron pool in human hematopoietic cells. *Cytometry A* 73:22–27.
- Wimpenny I, H Markides and AJ El Haj. (2012). Orthopaedic applications of nanoparticle-based stem cell therapies. *Stem Cell Res Ther* 3:13.
- Svanvik T, HB Henriksson, C Karlsson, M Hagman, A Lindahl and H Brisby. (2010). Human disk cells from degenerated disks and mesenchymal stem cells in co-culture result in increased matrix production. *Cells Tissues Organs* 191:2–11.
- Liu W and JA Frank. (2009). Detection and quantification of magnetically labeled cells by cellular MRI. *Eur J Radiol* 70:258–264.
- El Haj AJ, JR Glossop, HS Sura, MR Lees, B Hu, S Wolbank, M van Griensven, H Redl and J Dobson. (2012). An in vitro model of mesenchymal stem cell targeting using magnetic particle labelling. *J Tissue Eng Regen Med* [Epub ahead of print]; DOI: 10.1002/term.1636.
- Grootendorst DJ, J Jose, RM Fratila, M Visscher, AH Velders, B Ten Haken, TG Van Leeuwen, W Steenbergen, S Manohar and TJ Ruers. (2013). Evaluation of superparamagnetic iron oxide nanoparticles (Endorem(R)) as a photoacoustic contrast agent for intra-operative nodal staging. *Contrast Media Mol Imaging* 8:83–91.
- Qi Y, G Feng, Z Huang and W Yan. (2013). The application of super paramagnetic iron oxide-labeled mesenchymal stem cells in cell-based therapy. *Mol Biol Rep* 40:2733–2740.
- Markides H, O Kehoe, RH Morris and AJ El Haj. (2013). Whole body tracking of superparamagnetic iron oxide nanoparticle-labelled cells—a rheumatoid arthritis mouse model. *Stem Cell Res Ther* 4:126.
- Jing XH, L Yang, XJ Duan, B Xie, W Chen, Z Li and HB Tan. (2008). In vivo MR imaging tracking of magnetic iron oxide nanoparticle labeled, engineered, autologous bone marrow mesenchymal stem cells following intra-articular injection. *Joint Bone Spine* 75:432–438.

22. Arbab AS, GT Yocum, H Kalish, EK Jordan, SA Anderson, AY Khakoo, EJ Read and JA Frank. (2004). Efficient magnetic cell labeling with protamine sulfate complexed to ferumoxides for cellular MRI. *Blood* 104:1217–1223.
23. Wang HH, YX Wang, KC Leung, DW Au, S Xuan, CP Chak, SK Lee, H Sheng, G Zhang, et al. (2009). Durable mesenchymal stem cell labelling by using polyhedral superparamagnetic iron oxide nanoparticles. *Chemistry* 15: 12417–12425.
24. Singh H, J Reed, S Noble, JL Cangiano and DB Van Wyck. (2006). Effect of intravenous iron sucrose in peritoneal dialysis patients who receive erythropoiesis-stimulating agents for anemia: a randomized, controlled trial. *Clin J Am Soc Nephrol* 1:475–482.
25. Barot BS, PB Parejiya, DM Mehta, PK Shelat and GB Shah. (2013). Physicochemical and structural characterization of iron-sucrose formulations: a comparative study. *Pharm Dev Technol* 19:513–520.
26. Wagner W, R Saffrich and AD Ho. (2008). The stromal activity of mesenchymal stromal cells. *Transfus Med Hemother* 35:185–193.
27. Karlsson C, C Brantsing, T Svensson, H Brisby, J Asp, T Tallheden and A Lindahl. (2007). Differentiation of human mesenchymal stem cells and articular chondrocytes: analysis of chondrogenic potential and expression pattern of differentiation-related transcription factors. *J Orthop Res* 25:152–163.
28. Johnstone B, TM Hering, AI Caplan, VM Goldberg and JU Yoo. (1998). In vitro chondrogenesis of bone marrow-derived mesenchymal progenitor cells. *Exp Cell Res* 238: 265–272.
29. Tallheden T, M Brittberg, L Peterson and A Lindahl. (2006). Human articular chondrocytes—plasticity and differentiation potential. *Cells Tissues Organs* 184:55–67.
30. Tallheden T, C Karlsson, A Brunner, J Van Der Lee, R Hagg, R Tommasini and A Lindahl. (2004). Gene expression during redifferentiation of human articular chondrocytes. *Osteoarthritis Cartilage* 12:525–535.
31. Dehne T, R Schenk, C Perka, L Morawietz, A Pruss, M Sittlinger, C Kaps and J Ringe. (2010). Gene expression profiling of primary human articular chondrocytes in high-density micromasses reveals patterns of recovery, maintenance, re- and dedifferentiation. *Gene* 462:8–17.
32. Jarocho D, E Lukasiewicz and M Majka. (2008). Advantage of mesenchymal stem cells (MSC) expansion directly from purified bone marrow CD105+ and CD271+ cells. *Folia Histochem Cytobiol* 46:307–314.
33. Dominici M, K Le Blanc, I Mueller, I Slaper-Cortenbach, F Marini, D Krause, R Deans, A Keating, D Prockop and E Horwitz. (2006). Minimal criteria for defining multipotent mesenchymal stromal cells. International Society for Cellular Therapy position statement. *Cytotherapy* 8:315–317.
34. Jones EA, SE Kinsey, A English, RA Jones, L Straszynski, DM Meredith, AF Markham, A Jack, P Emery and D McGonagle. (2002). Isolation and characterization of bone marrow multipotential mesenchymal progenitor cells. *Arthritis Rheum* 46:3349–3360.
35. Dvorakova J, A Hrubá, V Velebný and L Kubala. (2008). Isolation and characterization of mesenchymal stem cell population entrapped in bone marrow collection sets. *Cell Biol Int* 32:1116–1125.
36. Delorme B and P Charbord. (2007). Culture and characterization of human bone marrow mesenchymal stem cells. *Methods Mol Med* 140:67–81.
37. Buhning HJ, S Treml, F Cerabona, P de Zwart, L Kanz and M Sobiesiak. (2009). Phenotypic characterization of distinct human bone marrow-derived MSC subsets. *Ann N Y Acad Sci* 1176:124–134.
38. Horwitz EM, K Le Blanc, M Dominici, I Mueller, I Slaper-Cortenbach, FC Marini, RJ Deans, DS Krause and A Keating. (2005). Clarification of the nomenclature for MSC: The International Society for Cellular Therapy position statement. *Cytotherapy* 7:393–395.
39. Chimal-Monroy J, J Rodriguez-Leon, JA Montero, Y Ganan, D Macias, R Merino and JM Hurle. (2003). Analysis of the molecular cascade responsible for mesodermal limb chondrogenesis: Sox genes and BMP signaling. *Dev Biol* 257:292–301.
40. Archer CW and P Francis-West. (2003). The chondrocyte. *Int J Biochem Cell Biol* 35:401–404.
41. Goldring MB, K Tsuchimochi and K Ijiri. (2006). The control of chondrogenesis. *J Cell Biochem* 97:33–44.
42. Heinegard D and A Oldberg. (1989). Structure and biology of cartilage and bone matrix noncollagenous macromolecules. *FASEB J* 3:2042–2051.
43. Hasty KA, GN Smith, Jr. and AH Kang. (1983). Histochemical identification of sulfation position in chondroitin sulfate in various cartilages. *J Histochem Cytochem* 31: 1367–1374.
44. Melrose J, SM Smith, RC Appleyard and CB Little. (2008). Aggrecan, versican and type VI collagen are components of annular translamellar crossbridges in the intervertebral disc. *Eur Spine J* 17:314–324.
45. Hasty KA, GN Smith, Jr. and AH Kang. (1981). Studies on glycosaminoglycans of regenerating rabbit ear cartilage. *Dev Biol* 86:198–205.
46. Metz S, G Bonaterra, M Rudelius, M Settles, EJ Rummeny and HE Daldrop-Link. (2004). Capacity of human monocytes to phagocytose approved iron oxide MR contrast agents in vitro. *Eur Radiol* 14:1851–1858.
47. Hansen HA and A Weinfeld. (1959). Hemosiderin estimations and sideroblast counts in the differential diagnosis of iron deficiency and other anemias. *Acta Med Scand* 165: 333–356.
48. Moewis G. (ed.). (1978). *Histopatologisk teknik*. Almqvist&Wiksell, Uppsala, 216 p.
49. Scott JE, G Quintarelli and MC Dellovo. (1964). The chemical and histochemical properties of Alcian Blue. I. The mechanism of Alcian Blue staining. *Histochemie* 4:73–85.
50. Goldstein DJ and RW Horobin. (1974). Surface staining of cartilage by Alcian blue, with reference to the role of microscopic dye aggregates in histological staining. *Histochem J* 6:175–184.
51. Al-Soud WA and P Radstrom. (2001). Purification and characterization of PCR-inhibitory components in blood cells. *J Clin Microbiol* 39:485–493.
52. Hedman J and P Radstrom. (2013). Overcoming inhibition in real-time diagnostic PCR. *Methods Mol Biol* 943:17–48.
53. Vogel V and MP Sheetz. (2009). Cell fate regulation by coupling mechanical cycles to biochemical signaling pathways. *Curr Opin Cell Biol* 21:38–46.
54. Yim EK and MP Sheetz. (2012). Force-dependent cell signaling in stem cell differentiation. *Stem Cell Res Ther* 3:41.
55. Kostura L, DL Kraitchman, AM Mackay, MF Pittenger and JW Bulte. (2004). Feridex labeling of mesenchymal stem cells inhibits chondrogenesis but not adipogenesis or osteogenesis. *NMR Biomed* 17:513–517.

56. Heymer A, D Haddad, M Weber, U Gbureck, PM Jakob, J Eulert and U Noth. (2008). Iron oxide labelling of human mesenchymal stem cells in collagen hydrogels for articular cartilage repair. *Biomaterials* 29:1473–1483.
57. Farrell E, P Wielopolski, P Pavljasevic, S van Tiel, H Jahr, J Verhaar, H Weinans, G Krestin, FJ O'Brien, G van Osch and M Bernsen. (2008). Effects of iron oxide incorporation for long term cell tracking on MSC differentiation in vitro and in vivo. *Biochem Biophys Res Commun* 369:1076–1081.
58. Balakumaran A, E Pawelczyk, J Ren, B Sworder, A Chaudhry, M Sabatino, D Stroncek, JA Frank and PG Robey. (2010). Superparamagnetic iron oxide nanoparticles labeling of bone marrow stromal (mesenchymal) cells does not affect their “stemness”. *PLoS One* 5:e11462.
59. Thu MS, LH Bryant, T Coppola, EK Jordan, MD Budde, BK Lewis, A Chaudhry, J Ren, NR Varma, AS Arbab and JA Frank. (2012). Self-assembling nanocomplexes by combining ferumoxytol, heparin and protamine for cell tracking by magnetic resonance imaging. *Nat Med* 18:463–467.
60. Foldager CB, M Pedersen, S Ringgaard, C Bunger and M Lind. (2011). Chondrocyte gene expression is affected by very small iron oxide particles-labeling in long-term in vitro MRI tracking. *J Magn Reson Imaging* 33:724–730.
61. Markoulatos P, N Siafakas and M Moncany. (2002). Multiplex polymerase chain reaction: a practical approach. *J Clin Lab Anal* 16:47–51.
62. Barreto H Henriksson, A Lindahl, E Skioldebrand, K Junevik, C Tangemo, J Mattsson and H Brisby. (2013). Similar cellular migration patterns from niches in intervertebral disc and in knee joint regions detected by in situ labeling: an experimental study in the New Zealand white rabbit. *Stem Cell Res Ther* 4:104.

Address correspondence to:  
*Helena Barreto Henriksson, PhD*  
*Department of Orthopaedics*  
*Sahlgrenska University Hospital*  
*Göteborg, SE 413 45*  
*Sweden*

*E-mail:* helena.barreto.henriksson@gu.se

Received for publication March 25, 2014

Accepted after revision July 15, 2014

Prepublished on Liebert Instant Online July 18, 2014